Developmental Biology 350 (2011) 323–336

Contents lists available at ScienceDirect

Developmental Biology

journal homepage: www.elsevier.com/developmentalbiology

Shox2 function couples neural, muscular and skeletal development in the proximal forelimb

Lori Vickerman, Stanley Neufeld, John Cobb *

Department of Biological Sciences, 2500 University Drive N.W., University of Calgary, Calgary AB T2N 1N4 Canada

ARTICLE INFO

Article history:
Received for publication 25 June 2010
Revised 13 November 2010
Accepted 29 November 2010
Available online 13 December 2010

Keywords:
Limb development
Axonal pathfinding
Muscle patterning
Shox2
Mup1
Epha7

ABSTRACT

The mouse *Shox2* gene codes for a homeodomain transcription factor that is required to form the proximal bones of the limbs, the humerus and femur. *Shox2* is the only gene known to be essential for the specific development of these skeletal elements. *Shox2* is also of special interest because it is closely related to the human *SHOX* gene, deficiencies of which cause the short stature in Turner, Langer and Léri–Weill syndromes. In order to understand in more detail the development of the proximal limb, we searched for *Shox2*-dependent gene expression patterns using Affymetrix microarrays. We compared the mRNA of *Shox2*-mutant and wild-type forelimb buds at 10.5 and 11.5 days of embryonic development (E10.5 and E11.5) and successfully identified a set of genes whose wild-type expression pattern requires *Shox2* function, as confirmed by in situ hybridization for eleven of the candidates. Strikingly, several of the identified genes were predicted to have functions in tissues other than the skeleton, including nerves and muscle precursors, prompting us to analyze neural and muscular patterning in *Shox2* mutants. We report here an axonal migration defect in *Shox2* mutants resulting in a profound innervation deficiency of the dorsal forelimb, including the complete absence of the radial and axillary nerves. Muscular development was also altered as early as E11.5. Specifically, the triceps muscles that develop along the posterior face of the humerus had severe abnormalities. These data demonstrate that *Shox2* is required for normal skeletal, neural and muscular development in the forelimb at a similar early developmental stage in each tissue.

Introduction

During embryonic development, the mouse forelimb is transformed from a bud of undifferentiated mesenchyme and overlying ectoderm into a structure with patterned skeletal, muscular and neural tissues. The patterning process happens in a proximal to distal sequence with the cells in the region of the humerus differentiating first followed by the radius/ulna domains and eventually the digits (Martin, 1990). The development of the skeleton has been the primary focus of studies that have established the tetrapod limb as a classical system for studying morphogenesis (Zeller et al., 2009). Mesenchymal cells of the bud condense and differentiate into chondrocytes that secrete the cartilage matrix to form the models of the mature bones. Simultaneously, muscle precursor cells that have migrated into the limb from the dermomyotome of the somites begin to differentiate and coalesce into muscle bundles (Duprez, 2002). The patterning of the somitic derivatives to form particular muscles is determined after their arrival in the limb bud as they are exposed to extrinsic signals in the mesenchyme (Hutcheson et al., 2009; Kardon et al., 2002). Meanwhile axons from motor and sensory neurons innervate the limb in a stereotyped pattern from their point of convergence near the base of the forelimb at the site of the future brachial plexus. Extrinsic signals guide the axons as they enter the limb bud; including the ephrins of the limb mesenchyme that interact with axonal Eph receptors (Luria et al., 2008). The axons that innervate the limb and the progenitors that form the muscles must pass through the proximal limb on their way to more distal domains. Despite its importance, the development of the proximal limb has been relatively understudied compared to the more distal elements. We understand little about how skeletal, muscular and neural patterning is coordinated, even though their coupling is required for the development of a functional limb.

Transcription factors are expected to be involved in integrating the diverse patterning processes in the limb since they simultaneously control the localized expression patterns of a variety of downstream genes (Cobb and Duboule, 2005; Salsi et al., 2008). However, with few exceptions (e.g. Hasson et al., 2010), functional studies of transcription factors during limb development have focused on the skeleton. The clustered *Hox* genes are the most studied transcription factors that pattern the limbs, although other homeobox genes have prominent roles (Tickle, 2003; Zakany and Duboule, 2007). The patterning of the proximal limb has been attributed to the HOX proteins of the 9 and 10 paralogous groups (Davis et al., 1995; Wellik and Capecchi, 2003) and to the MEIS1 and MEIS2 homeodomain

* Corresponding author. Fax: +1 403 289 9311.
E-mail address: jacobb@ucalgary.ca (J. Cobb).

0012-1606/$ – see front matter © 2010 Elsevier Inc. All rights reserved.
doi:10.1016/j.ydbio.2010.11.031

proteins (Mercader et al., 1999; Tickle, 2003; Zeller et al., 2009). Simultaneous inactivation of all three *Hox10* paralogs resulted in mice with no femur but the corresponding element in the forelimb, the humerus, was still present (Wellik and Capecchi, 2003). Since *Hoxa9*/*Hoxd9*-mutant mice develop with a shortened humerus it was suggested that both *Hox10* and *Hox9* paralogs are required to pattern the proximal forelimb, thus accounting for the presence of a humerus in the *Hox10* triple knockout animals. Nonetheless, no combination of *Hox* mutations has yet been described that completely eliminates the humerus. Indeed, a portion of the humerus still developed when all *HoxA* and *HoxD* function was removed from the forelimbs of mice by deleting both of these complexes (Kmita et al., 2005).

The function of the *Meis* genes in the proximal limb is supported by experiments in which *Meis1* misexpression in chick embryos caused distal-to-proximal transformations (Mercader et al., 1999). Similarly, misexpression of *Meis1* in the distal domains of developing mouse limbs disrupted patterning, although it was unclear if this constituted proximalization (Mercader et al., 2009). A definitive determination of the role of *Meis* genes in mouse limb development will likely require the generation of *Meis1*/*Meis2* double mutants, since *Meis1*-null mice have no obvious limb defects (Hisa et al., 2004). Therefore, *Hox* and *Meis* mutants have not provided a specific model for studying the development of the proximal limb to date.

In contrast, mutation of the Short-stature homeobox 2 gene (*Shox2*) caused a limb phenotype remarkably similar to that predicted for inactivation of the *Meis* and *Hox9*/*10* genes, perhaps reflecting a function for *Shox2* downstream of these genes. Conditional deletion of *Shox2* in limbs resulted in the virtual absence of a humerus and femur in mutant animals, while the distal limb was relatively unaffected (Cobb et al., 2006). Therefore the *Shox2* mutant is currently the best model for specific study of proximal limb development. We linked the *Shox2*-mutant skeletal phenotype to a lack of *Runx2* expression and a corresponding delay of chondrocyte maturation in the developing humerus. Before the current study, the downregulation of *Runx2* at E11.5 was the earliest known differentially expressed gene in *Shox2*-mutant limbs (Cobb et al., 2006).

The limb defects are probably so severe in *Shox2*-mutants because mice have lost the second Short-stature homeobox paralog, *Shox*, found in other vertebrates. Mice lack the *Shox* gene because a segment of the pseudoautosomal region of the sex chromosomes, which includes the *Shox* locus, was lost during evolution (Graves et al., 1998). Haploinsufficiency of *SHOX* causes short stature in humans with Turner and Léri–Weill syndromes, and homozygous deficiency causes the more severe limb deformities of Langer syndrome (Rao et al., 1997; Shears et al., 1998; Zinn et al., 2002). In all of these conditions, the forearms and lower legs (the zeugopod elements) are shortened and often misshapen; therefore, the phenotype of human *SHOX* patients is similar to *Shox2*-mutant mice except that a different proximodistal segment is affected. Humans also have a *SHOX2* gene but no mutations of this gene have yet been reported (Blaschke et al., 1998; Semina et al., 1998). The mouse SHOX2 protein is 79% identical to human SHOX and 99% identical to human SHOX2; the DNA-binding homeodomains of all three proteins are 100% identical (Clement-Jones et al., 2000). Therefore, because of the similarity of the proteins and mutant phenotypes, the study of mouse *Shox2* will likely help elucidate the function of human *SHOX* and *SHOX2*.

In the current study we used microarrays to compare the transcriptomes of control and *Shox2*-mutant embryonic forelimb buds to gain further insight into the developmental processes controlled by *Shox2*. We identified differential gene expression patterns that indicated altered neural and muscular development in *Shox2* mutants, and we report axonal pathfinding and muscle developmental defects in limbs lacking *Shox2* function. These data demonstrate a *Shox2*-dependent coupling of skeletal, neural and muscular development in the proximal forelimb. To our knowledge this is the first time one transcription factor has been shown to mediate the patterning of three tissue types during the early stages of limb development.

Materials and methods

Mice, tissue samples and RNA extraction

As previously described (Cobb et al., 2006), we generated embryos in which *Shox2* was deleted either in all tissues ($Shox2^{-/-}$) or conditionally deleted in developing limbs ($Prx1\text{–}Cre;Shox2^{floxed/-}$ hereafter referred to as $Shox2^{c/-}$). Mice were maintained on a mixed C57BL/6–129/Sv background. Wild type and heterozygote embryos were used interchangeably as controls since we have never detected any abnormalities in heterozygote ($Shox2^{+/-}$) animals, which are viable, fertile and have limbs that are indistinguishable from wild type (Cobb et al., 2006). Mutant embryos at E10.5 were either $Shox2^{c/-}$ or $Shox2^{-/-}$. All E11.5 embryos used were conditional $Shox2^{c/-}$ mutants, since at that stage $Shox2^{-/-}$ embryos die from a heart defect (Blaschke et al., 2007; Cobb et al., 2006). Noon on the day of plugging was assumed to be E0.5. We counted somites for more precise staging: 34–37 somite embryos were used for E10.5 tissue samples and 45–50 somites for E11.5. Forelimb buds were dissected with a tungsten needle at the body wall. For E10.5 microarray samples the entire limb bud was used. For E11.5 samples, the most distal portion of the limb bud was removed with fine forceps, as indicated in Fig. 1C. Tissue samples were stored in RNAlater (Qiagen) at −20 °C during genotyping.

Forelimb buds from two to three embryos of the same genotype were pooled and homogenized with a Polytron device using the Qiagen RLT solution. RNA was purified using an RNeasy mini kit (Qiagen). 3–14 μg of RNA was isolated from each of three biological replicate samples for each stage and genotype. RNA quality was confirmed with a 2100 Bioanalyzer (Agilent).

U. Drescher provided $Epha7^{-/-}$ embryos. This mutant line was described previously (Rashid et al., 2005).

Microarray hybridization and analysis

For each of twelve samples, 1 μg of RNA was used to synthesize biotinylated cRNA with the MessageAmp II-Biotin Enhanced Kit (Ambion). cRNA was then hybridized to a total of 12 Affymetrix Mouse Genome 430 2.0 oligonucleotide arrays according to the manufacturer's protocol. Data from scanned microarrays was analyzed with Affymetrix GCOS 1.2 software to identify differentially expressed transcripts by pairwise comparisons as described (Le Martelot et al., 2009). For both the E10.5 and E11.5 time points, each of three control samples was compared to each of three mutant samples for a total of nine pairwise comparisons per time point. This method is based on the Mann–Whitney pairwise comparison test and allows the ranking of results by concordance, as well as the calculation of significance (p-value) for each identified change in gene expression (Hubbell et al., 2002; Liu et al., 2002). Genes for which the concordance in the pairwise comparisons exceeded the imposed threshold of seven out of nine comparisons were considered statistically significant. In addition, we only considered transcripts whose accumulation had an average change of at least 1.4-fold. In a previous study we found that many genes with six of nine significant pairwise comparisons could also be confirmed as differentially expressed, although with a higher number of false positives (Cobb and Duboule, 2005). Therefore, selected genes in this category (e.g. *Epha7*) were selected for further analysis and verification. The microarray data were deposited in the ArrayExpress database with accession number E-MTAB-411.

We removed 5 genes from the list of E11.5 differentially expressed genes that are known to be sexually dimorphic: *Xist* was higher in the

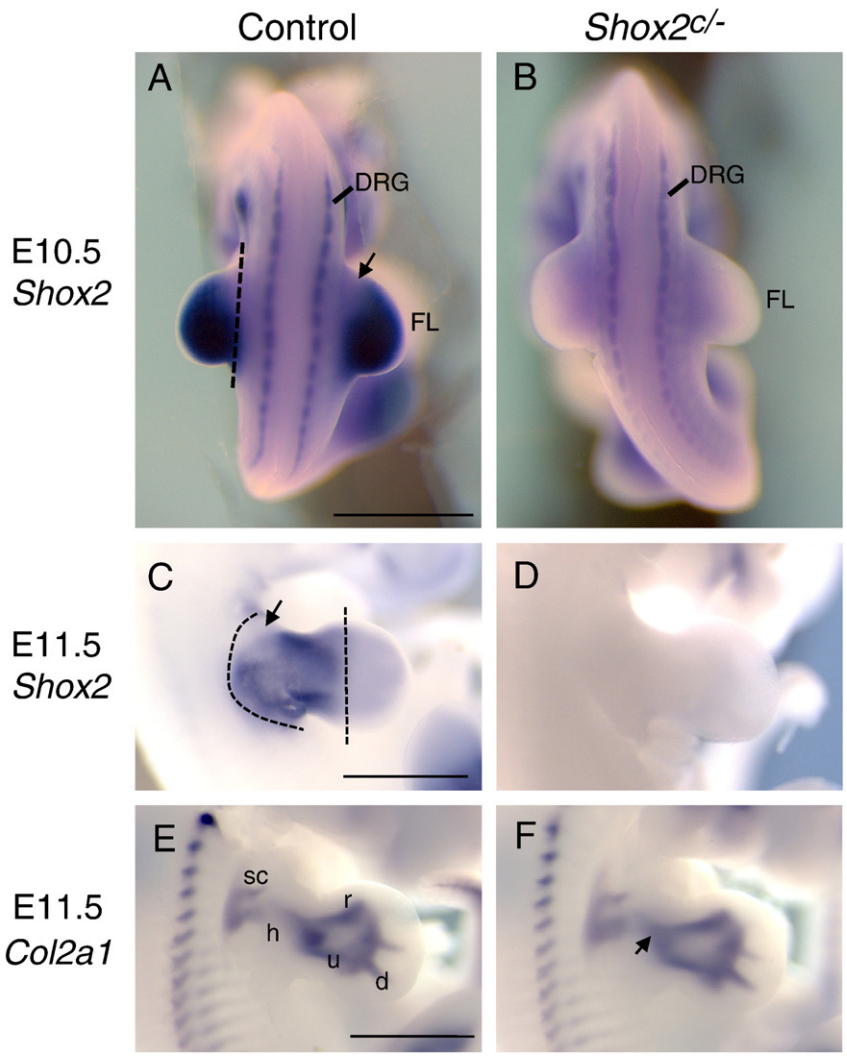

Fig. 1. *Shox2* and *Col2a1* expression in developing forelimb buds and samples taken for microarray analysis. (A–D) *Shox2* expression as revealed by WISH of wild-type and *Prx1-Cre; Shox2* conditional mutant embryos (*Shox2*$^{c/-}$) at E10.5 and E11.5. Dotted lines indicate the cut points for microdissection of samples used in the microarray experiment. DRG = dorsal root ganglia, FL = forelimb. (E–F) WISH for *Col2a1* indicates the location of immature chondrocytes of the forming limb elements: sc = scapula, h = humerus, r = radius, u = ulna, d = digits. The patterning is relatively normal in the mutant, which has only a slightly smaller humerus anlagen (arrow). Scale bars represent 1 mm.

control samples and four genes from the Y chromosome (*Ddx3y*, *Jarid1d*, *Uty*, and *Eif2s3y*) were higher in mutant samples. The detection of these genes indicates that more female embryos were present in the control samples at this time point, but all of these genes are known to be expressed in gonads before gonadal determination (Nef et al., 2005) so they presumably represent constitutive expression from the sex chromosomes before the appearance of sexually dimorphic characteristics.

In situ hybridization

All probes were generated by RT-PCR from cDNA produced from E10.5 or E11.5 limb bud RNA using Superscript II reverse transcriptase (Invitrogen) using primers listed in Supplementary Table 3. The cDNA fragments were cloned into the pGEMT vector (Promega) and their identity confirmed by restriction enzyme analysis. DIG labeled riboprobes were produced as described (Cobb et al., 2006). Whole-mount in situ hybridization (WISH) of embryos fixed overnight in 4% paraformaldehyde was performed according to standard procedures. Images show one representative staining of at least three replicates for each condition. When more than three replicates were performed that is indicated in the text. All pairs of images presented are from mutant and control embryos that were stained in the same well to assure identical experimental conditions.

Immunohistochemistry

Antibodies recognizing neurofilaments (2H3) and muscle myosin (MF20) were used to visualize embryonic nerves and muscles. An identical protocol was used for each antibody. Embryos were fixed at least 4 h in Dent's fixative (4:1, Methanol:DMSO). Embryos were bleached overnight in 5:1 Dent's fixative: 30% H_2O_2, then rehydrated with successive 30-minute washes in 50%/30%/0% Methanol in PBS–0.5% Tween (PBST). Embryos were blocked two times for 1 h in PBST/1% DMSO/2% skim milk powder (PBSTMD) then incubated overnight at 4 °C with primary antibody diluted 1:50–1:150 in PBSTMD. Embryos were then washed four times for 1 h with PBST, reblocked with PBSTMD, and incubated overnight with peroxidase-conjugated goat anti-mouse IgG (Sigma A-9169) diluted 1:300 in PBSTMD, then washed as before, stained with DAB (diaminobenzidine) and 0.003% H_2O_2, dehydrated to 100% Methanol and cleared in BABB (1:2, benzyl alcohol:benzyl benzoate).

The 2H3 and MF20 antibodies were developed by T. Jessell/J. Dodd (Dodd et al., 1988) and D. Fischman (Bader et al., 1982), respectively and were obtained from the Developmental Studies Hybridoma Bank

developed under the auspices of the NICHD and maintained by The University of Iowa, Department of Biology, Iowa City, IA 52242.

Results

Our goal was to identify developmental pathways regulated by *Shox2* in embryonic limbs. Toward this end, we used Affymetrix microarrays to compare gene expression in control and *Shox2*-mutant forelimb buds at E10.5 and E11.5. We focused on these stages because this is when differentiation is commencing in the limb bud and pattern emerges. We chose the E10.5 time point to maximize chances of identifying the earliest expression changes dependent on *Shox2* since this is when the gene is first robustly expressed (Meijlink et al., 1999), as shown by WISH in Fig. 1A. At E10.5, *Shox2* transcripts were detected throughout the limb bud mesenchyme except for a small anterior domain (Fig. 1A). A second time point at E11.5 was included to determine which expression changes persisted and which new ones appear at this later stage. At E11.5 *Shox2* expression became restricted to the proximal limb in a domain corresponding to the developing stylopod (humerus) and zeugopod (radius and ulna) elements, as can be seen by comparing *Shox2* and *Col2a1* expression in Figs. 1C and E respectively. Tissue samples were dissected to approximate these domains as indicated by the dashed lines in Figs. 1A and C. Importantly, both stages used in this study are before morphological changes are readily visible; thus any changes in gene expression should reflect early patterning processes before drastically altered structures are present and many secondary gene expression differences would be expected. Abnormalities in the mutant skeleton are only apparent at E11.5 if chondrocyte markers are analyzed to reveal a slightly smaller humerus condensation of *Col2a1*-expressing chondrocytes (Fig. 1F). Severe abnormalities appear in the skeleton after E11.5 because of a defect in chondrocyte maturation as revealed by a lack of *Runx2* (runt related transcription factor 2) expression (Cobb et al., 2006).

Expression profiling identifies genes with Shox2-dependent expression

RNA samples from *Shox2*-mutant and control forelimb buds were compared using whole genome Affymetrix oligonucleotide microarrays with probesets representing more than 39,000 transcripts. We analyzed triplicate samples to give a total of nine pairwise comparisons for each time point. Tables 1–3 show all genes that met the stringent requirement of at least seven significantly different pairwise comparisons and a greater than 1.4-fold change in expression. As expected *Shox2* showed the largest fold-changes (85 to 240-fold) and is not included in the tables. Using these criteria, six differentially expressed genes were found at E10.5 and seventeen at E11.5 with fold changes from 1.4 to 14 fold. Among these candidates only three genes, *Mup1* (major urinary protein 1), *Rspo3* (R-spondin 3) and *Igf1* (insulin-like growth factor 1), were significantly different at both developmental stages. This list is likely an underestimate of differentially expressed genes, particularly since *Runx2*, which we previously identified as downstream of *Shox2* by a candidate gene approach (Cobb et al., 2006), was only included if the criteria were relaxed to include genes with six significant pairwise comparisons (Supplementary Tables 1 and 2). Therefore, Tables 1–3 show the genes for which the changes have the most statistical significance but are not expected to be comprehensive.

As a first step in understanding the significance of the genes identified by the microarray analysis, we validated differential expression by WISH. As shown previously for *Runx2* (Cobb et al., 2006), the spatial expression pattern revealed by WISH can be more informative than a numeric fold-change value, particularly when the expression change is confined to a small, but morphologically significant domain. We selected fifteen genes (shown in bold in Tables 1–3) for in situ analysis with a particular emphasis on the three

Table 1
Differentially expressed genes at E10.5.

Gene symbol	Function and/or cellular location as indicated by selected GO terms[a]	Affymetrix probe set ID	Fold change	Significant pairwise comparisons, N/9[b]
*A. Genes with **higher** expression in Shox2-mutant forelimbs*				
Mup1	Pheromone binding; transport activity	1426154_s_at	6.10	9
Mup1		1430893_at	4.49	9
Mup1		1420465_s_at	4.39	9
Rspo3	Canonical Wnt receptor signaling pathway; frizzled binding	1455607_at	1.43	9
*B. Genes with **lower** expression in Shox2-mutant forelimbs*				
Tiparp	NAD + ADP-ribosyltransferase activity	1452161_at	−1.56	9
H2-D1	Antigen processing and presentation	1425545_x_at	−1.63	7
Igf1	Insulin-like growth factor receptor binding; positive regulation of cell growth	1434413_at	−1.61	7
Cxcr7	G-protein coupled receptor activity; integral to membrane	1417625_s_at	−1.42	7

[a] Gene ontology (GO) terms from the Mouse Genome Informatics Database (http://www.informatics.jax.org/; Bult et al., 2010).
[b] Number of 9 pairwise comparisons showing significant increase or decrease ($p<0.0025$) by Wilcoxon's Signed Rank Test.

Table 2
Genes with higher expression in *Shox2*-mutant forelimbs at E11.5.

Gene symbol	Function and/or cellular location as indicated by selected GO terms	Affymetrix probe set ID	Fold change	Significant pairwise comparisons, N/9[a]
Mup1	Pheromone binding; transport activity	1420465_s_at	14.61	9
Mup1		1430893_at	8.99	9
Mup1		1426154_s_at	8.58	9
Lmo1	Metal-ion binding; nucleus	1418478_at	1.89	9
Rspo3	Canonical Wnt receptor signaling pathway; frizzled binding	1455607_s_at	1.59	9
Dmd	Actin binding; skeletal muscle tissue development; plasma membrane	1448665_at	1.53	9
Dmd		1417307_at	1.48	9
Mlf1	DNA-binding; myeloid progenitor cell differentiation	1418589_a_at	1.52	9
Prrx1	Sequence-specific DNA binding transcription factor activity	1425527_at	1.51	9
Rsrc1	Alternative nuclear mRNA splicing	1448584_at	1.40	9
Gria2	Ionotropic glutamate receptor activity; integral to membrane	1421970_a_at	1.69	8
Osr2	Transcription factor activity; bone morphogenesis	1426155_a_at	1.49	8
C1QL3	Protein binding; intracellular region	1451620_at	2.05	7
Rarres1	Proteinase inhibitor, latexin domain	1438055_at	1.78	7
Epha7[b]	Ephrin receptor activity; branching morphogenesis of a nerve	1452380_at	1.71	6

[a] Number of 9 pairwise comparisons showing significant increase or decrease ($p<0.0025$) by Wilcoxon's Signed Rank Test.
[b] Although *Epha7* and *Runx2* showed significant differential expression in only 6 pairwise comparisons, they are included here because their differential expression was conclusively demonstrated by in situ hybridization.

Table 3
Genes with lower expression in *Shox2*-mutant forelimbs at E11.5.

Gene symbol	Function and/or cellular location as indicated by selected GO terms	Affymetrix probe set ID	Fold change	Significant pairwise comparisons, N/9[a]
Lect1	Negative regulation of angiogenesis; cartilage development; integral to membrane	1460258_at	−1.91	8
Matn4	Extracellular region; EGF-like region	1418464_at	−2.47	7
Ednrb	Endothelin receptor activity; peripheral nervous system development	1437347_at	−1.81	7
Meox1	Sequence-specific DNA-binding transcription factor activity; somite specification	1417595_at	−1.78	7
Postn	Cell adhesion; extracellular region	1423606_at	−1.64	7
Igf1	Insulin-like growth factor receptor binding; positive regulation of cell growth	1437401_at	−1.47	7
Igf1		1434413_at	−1.45	7
Runx2[b]	Sequence-specific DNA-binding transcription factor activity; positive regulation of chondrocyte and osteoblast differentiation	1424704_at	−1.62	6

[a] Number of 9 pairwise comparisons showing significant increase or decrease ($p<0.0025$) by Wilcoxon's Signed Rank Test.
[b] Although *Epha7* and *Runx2* showed significant differential expression in only 6 pairwise comparisons, they are included here because their differential expression was conclusively demonstrated by in situ hybridization.

genes differentially expressed at both time points. Eleven of these fifteen showed clear expression differences by WISH (Figs. 2–5). The four genes for which differential expression was not confirmed by this method were either expressed at particularly low (*Mlf1* and *Tiparp*) or high (*Prrx1* and *Lmo1*) levels, perhaps indicating that their differential expression is outside of the dynamic range for detection by WISH (Supplementary Fig. 1).

Candidate genes with differential expression at both time points

At both E10.5 and E11.5, *Mup1* showed the largest differential expression by microarray analysis with three different probesets, and this was clearly confirmed by WISH (Figs. 2A–B, E–F). Interestingly, *Mup1* transcripts were detected in wild-type limbs, but only in a very small domain in the anterior limb at E10.5 (Fig. 2A, arrow) that corresponds to the area where *Shox2* transcripts were excluded (compare to arrow in Fig. 1A). In the *Shox2* mutant, this expression domain expanded dramatically (Fig. 2B), suggesting that *Shox2* is necessary to restrict *Mup1* expression to the anterior proximal limb. At E11.5, the gain of *Mup1* expression was confined to the area of the mesenchyme around the humerus anlagen (Fig. 2F, compare to Figs. 1E–F). We also detected *Mup1* transcripts in other tissues in control and mutant embryos, including the somites and otic vesicle (data not shown). Although the gain in *Mup1* expression was obvious at the mRNA level we were unable to detect MUP1 protein expression in limb buds by immunoblot analysis (data not shown).

As for *Mup1*, differential expression of *Rspo3* and *Igf1* was detected by microarray at both E10.5 and E11.5. Despite a lower fold-change than *Mup1*, an upregulation of *Rspo3* was also clearly validated by WISH at E10.5 and E11.5 (Figs. 2C–D, G–H). *Rspo3* expression was gained in the mutant in a domain along the posterior extent of the limb bud in a region where *Shox2* was expressed in the controls, suggesting that SHOX2 could be involved in limiting *Rspo3* expression in wild-type limbs. At E11.5, *Rspo3* remained upregulated in a central region of the limb bud also where *Shox2* was normally expressed (Figs. 2G–H, arrows). The downregulation of *Igf1* detected by microarray could only be confirmed at E11.5 (Figs. 2I–J), but was consistent in four of four E11.5 embryos tested. The loss of *Igf1* expression was seen in the proximal and posterior regions of the bud (arrow and arrowhead in Figs. 2I–J). We could not detect *Igf1* transcripts in limb buds at E10.5 (Supplementary Figs. 1A–B).

Extracellular matrix, neural and myogenic candidate genes

Matn4 (matrilin 4) had the second highest fold change (2.47-fold decrease in mutants) and was the only gene among all candidates coding for an extracellular matrix (ECM) protein (Tables 1–3). The general lack of ECM genes among the misexpressed transcripts was not surprising given that *Col2a1* expression is intact in the mutant humerus at this early stage (Fig. 1F). Therefore the effect on *Matn4* expression appears to be specific rather than reflecting a general failure to express components of the cartilage matrix. *Matn4* expression clearly marked the skeletal elements in control limbs (Fig. 3A). In the mutant, the humerus condensation lacked *Matn4* transcripts although the other limb elements showed normal *Matn4* expression (Fig. 3B).

Similarly, a deficiency of *Ednrb* (endothelin receptor type B) expression was noted in the region of the humerus of mutant embryos, but in this case the signal labeled axons of nerves innervating the limb. In the control limbs the radial and axillary nerves were visualized due to the presence of *Ednrb* transcripts (Fig. 3C). This staining could presumably be due the detection of axonal mRNA or expression in cells closely associated with the axons. This staining is consistent with the known expression of this gene in the neural tube and sensory neurons (Lee et al., 2003). In the mutant limbs there was a conspicuous lack of *Ednrb*-labeled axons in the dorsal limb (Fig. 3D). Instead, *Ednrb* expression appeared truncated at the base of the mutant limb where the radial and axillary nerves normally bifurcate (arrowhead in Figs. 3C–D). This staining was later found to indicate a lack of axons projecting into the dorsal limb, as discussed below. *Gria2* (glutamate receptor, ionotropic, AMPA2 (alpha 2), also known as *GluR-B*), another gene known to be expressed in neurons (Kask et al., 1998), was upregulated in the mesenchyme of the mutant proximal limb (Figs. 3E–F), but unlike *Ednrb*, the expression does not appear to correspond to axons.

The two candidate genes expressed in cells derived from somites had opposite responses to the lack of *Shox2*: *Dmd* was upregulated (Figs. 4A–B) and *Meox1* was downregulated in mutant limbs (Figs. 4C–D), both within the *Shox2* expression domain (compare to Fig. 1C). *Dmd*, which codes for the dystrophin protein, is expressed in somitic cells that have differentiated into skeletal muscle myocytes (Houzelstein et al., 1992). Therefore, its upregulation suggests a possible increase in myocytes in the stylopod region. In contrast, *Meox1* (mesenchyme homeobox 1) is expressed broadly in undifferentiated, epithelialized somites and appears in the limb bud at E11.5 in the region of the dorsal and ventral muscle masses (Reijntjes et al., 2007). This limb bud expression domain was largely absent in E11.5 mutant limbs (Figs. 4C–D). A similar decrease in *Lect1* (leukocyte cell derived chemotaxin 1) expression was seen in the proximal limb (Figs. 4E–F). *Lect1* codes for the chondromodulin protein that inhibits angiogenesis in the avascular zone of differentiating cartilage (Shukunami et al., 1999), suggesting that vascular patterning could also be altered in mutant limbs.

Interestingly, the two genes located nearest to *Shox2* on chromosome 3 were among those for which an expression increase was detected. The start site for *Rsrc1* (arginine/serine-rich coiled-coil 1), a gene of unknown function, is only about 4 kb upstream of *Shox2*, and this gene was clearly upregulated in the mutant limb in a *Shox2*-like

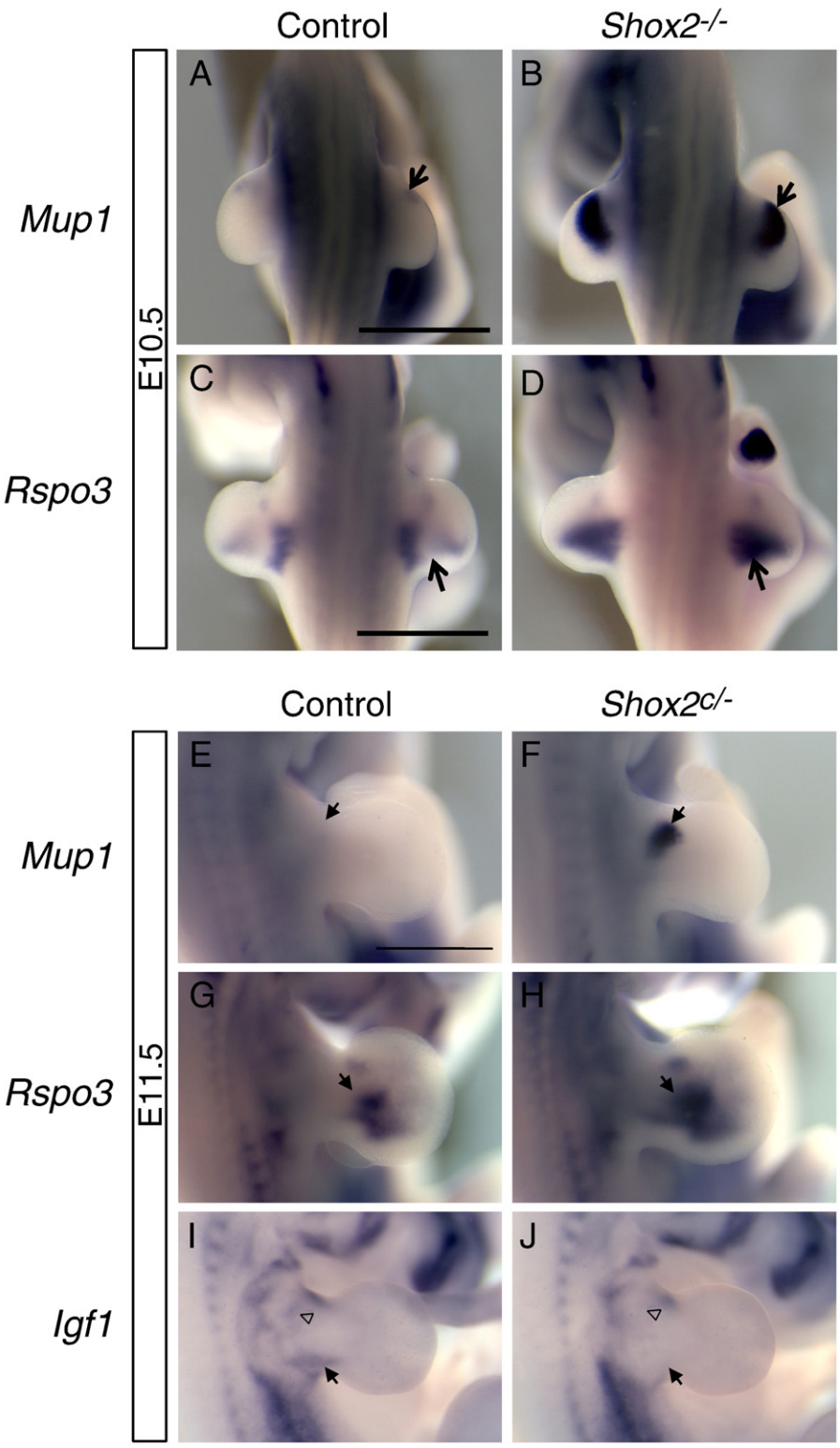

Fig. 2. Genes for which microarrays detected differential expression at both E10.5 and E11.5. (A–D) Images are dorsal views of either control or *Shox2*$^{-/-}$ E10.5 embryos hybridized with *Mup1* (A–B) or *Rspo3* (C–D) riboprobes. Arrows indicate the regions of the forelimb where expression is gained in the mutants. The control in A is *Shox2*$^{+/+}$ to confirm that *Mup1* is expressed in wild-type limbs; heterozygote expression appears identical (not shown). (E–J) All images are dorsal views of right forelimb buds of control or *Shox2*$^{c/-}$ E11.5 embryos at the same magnification, hybridized with the indicated riboprobes. Arrows indicate regions where staining is higher (*Mup1* and *Rspo3*) or lower (*Igf1*) in the mutants. Arrowheads in I–J indicate an additional region where *Igf1* expression is downregulated in the mutant. Scale bar represents 1 mm.

pattern (Figs. 4G–H). The next gene beyond *Rsrc1* is *Mlf1* (myeloid leukemia factor 1), 400 kb upstream of *Shox2*. An upregulation of this gene was also detected by the microarray analysis (Table 2), although this increase was not detected by WISH (Supplementary Figs. 1G–H). We speculate that the increase in *Rsrc1* and *Mlf1* may be attributed to cis-regulatory elements gaining access to other nearby promoters upon deletion of *Shox2*. While we cannot rule out that their misexpression contributes to the mutant phenotypes, the change in

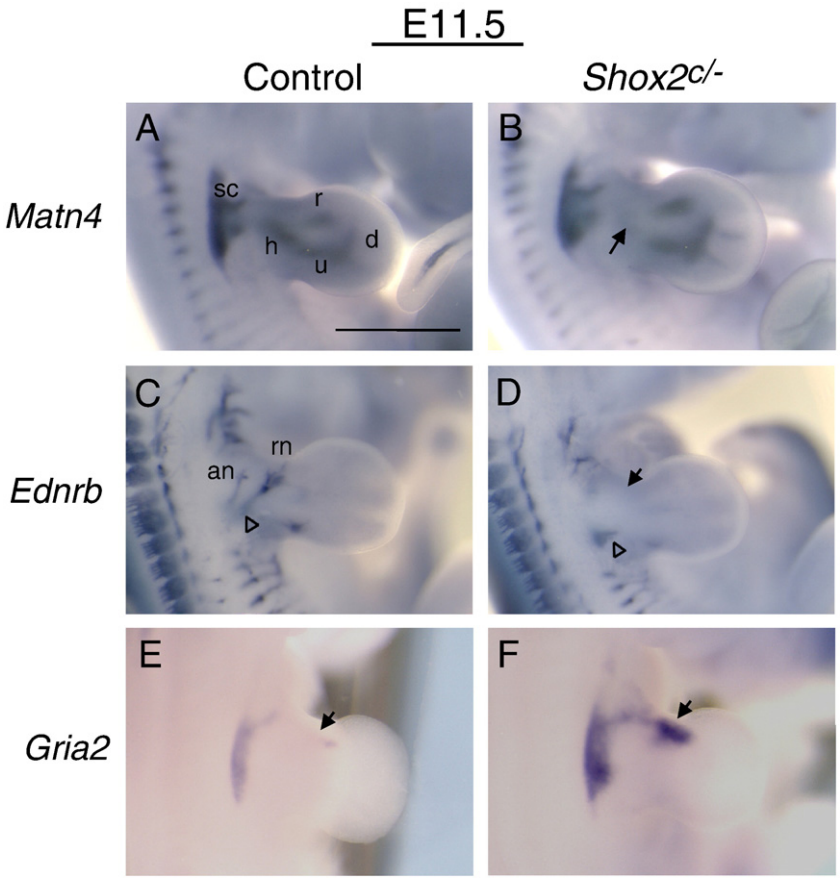

Fig. 3. Differentially expressed genes at E11.5 that are predicted to code for extracellular matrix or neural proteins. All images depict dorsal views of right forelimb buds at the same magnification, hybridized with the indicated riboprobes. Arrows indicate regions where staining is lower for *Matn4* and *Ednrb* (B, D) or higher for *Gria2* (F) in mutants. Arrowhead in C–D indicates where the neural staining is truncated in the mutant. rn = radial nerve. an = axillary nerve. Skeletal elements in A are labeled as in Fig. 1E. Scale bar represents 1 mm.

expression of *Rsrc1* and *Mlf1* most likely reflects an artifact of *Shox2* deletion.

Taken together, the expression patterns described here reveal substantial gene regulation defects in *Shox2* mutants. All of the expression differences are localized to the proximal region of the limb that includes both the humerus and radius/ulna domains, establishing this part of the limb bud as a center for *Shox2*-dependent gene expression.

Limb innervation defects in Shox2 mutants

We next wanted to determine if the loss of *Ednrb*-labeled axons in the dorsal limb of *Shox2* mutants was due to the selective loss of a subset of axons, or whether it reflected a more substantial innervation deficit. Therefore, we stained control and *Shox2* mutants with the 2H3 antibody that detects neurofilaments to visualize all nerves in the developing embryo (Fig. 5). In E11.5 control limbs, nerves could be seen extending into both the dorsal and ventral limb: the median and ulnar nerves innervated the ventral limb and the axillary and radial nerves innervated the dorsal domains (Figs. 5A and E). (Rodent embryonic neural anatomy is from Shearer (1933).) In the mutant limb the median and ulnar nerves appeared normal, but the *brachialis superior* was truncated as it failed to branch to produce the radial and axillary nerves (Figs. 5B and F). At later stages, the radial nerve in control limbs extended distally at E12.5 (Fig. 5I) and reached the digits by E13.5 (Fig. 5M). (Because of the limb defects of older $Shox2^{c/-}$ embryos, the limbs extend straighter from the body than in the controls, causing an unavoidable difference in perspective in mice of the two genotypes.) In mutants, the radial and axillary nerves remained absent at these later stages, leaving the dorsal limb almost completely devoid of innervation (Figs. 5J and N). The ventral limb was innervated normally in mutants, as can be seen by the median and ulnar nerves reaching the digits, out of focus in Fig. 5N. WISH with an *Ednrb* probe at E12.5 confirmed that the lack of *Ednrb* expression in the dorsal limbs of mutants correlated with the complete lack of the radial and axillary nerves in these regions (Figs. 5K–L). To further confirm the persistent lack of the radial nerve, we dissected the brachial plexus region of mutant and control weanlings. In five of five mutants there was no radial nerve present, while the radial nerve was obvious in control littermates (data not shown). Although this study focused on the forelimb, we noticed that the innervation of the hindlimb had no major abnormalities (see Discussion and Figs. 7C–D).

Next we sought to identify candidate molecules that might produce the axonal migration defect we identified in *Shox2* mutants. We examined our list for genes known to code for proteins involved in axonal pathfinding, such as ephrins and their receptors (Eph proteins). While no such genes were in our most stringent list, the more expanded gene set (Supplementary Tables 1 and 2), included an upregulation of the *Epha7* gene in mutant limbs at E11.5. WISH of E11.5 embryos confirmed the upregulation of *Epha7* in a dorsal domain of the proximal limbs of *Shox2* mutants (Figs. 5G–H). A posterior (side) view showed that the gain in expression was limited to the dorsal limb in the region where axonal migration was blocked (Figs. 5C–D). *Epha7* was expressed in this region in control limbs, but in a more restricted domain (Figs. 5C and G). Therefore *Shox2* could function to repress *Epha7* expression in the dorsal limb.

Mice null for *Epha7* have been generated previously and a disruption of the retinocollicular map was reported (Rashid et al., 2005). However, the limb innervation pattern in these mutants has not been described. Therefore we stained $Epha7^{-/-}$ embryos at E12.5

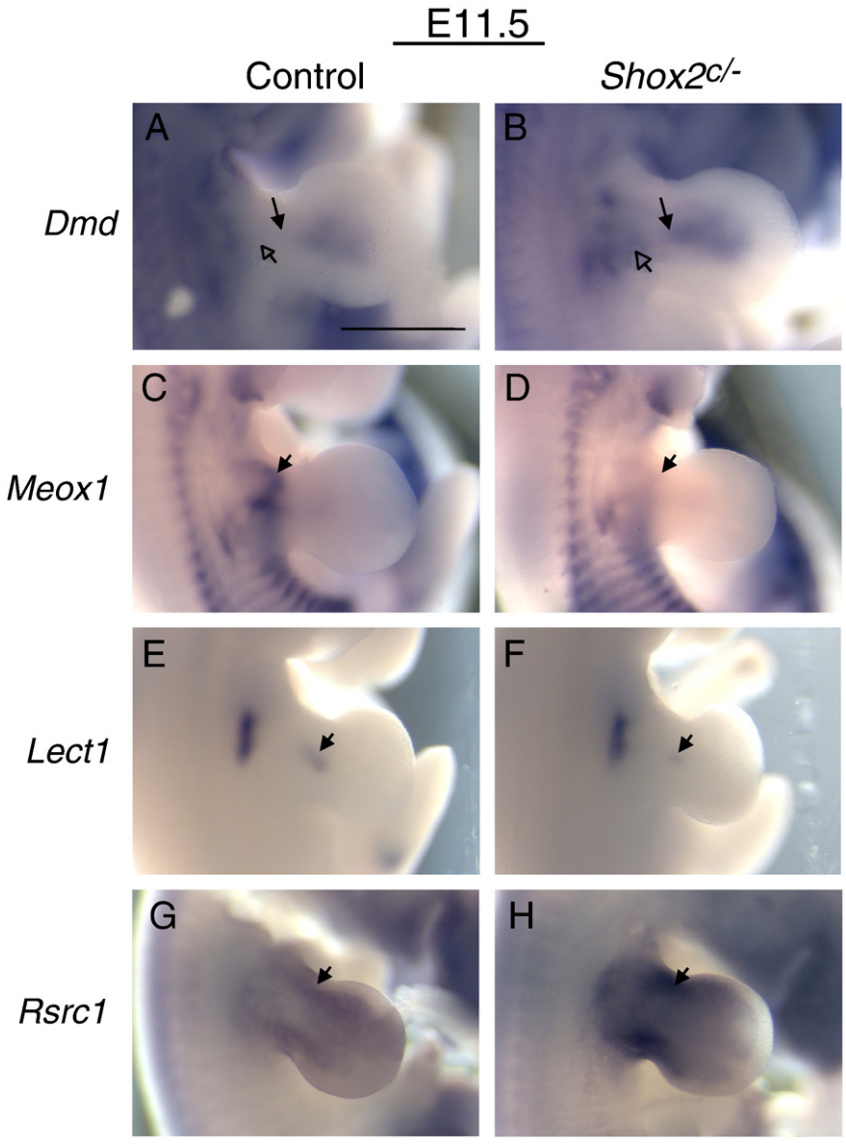

Fig. 4. Candidate genes expressed in somitic derivatives or other tissues. Images are as in Fig. 3. Arrows indicate regions where staining is higher (*Dmd* and *Rsrc1*) or lower (*Meox1* and *Lect1*) in mutant forelimbs.

with the 2H3 antibody. At this stage the radial and axillary nerves had similar patterns in mutant and wild type embryos (Supplementary Fig. 2). These results indicate that there is no absolute requirement for *Epha7* in limb innervation; however, they do not rule out possible effects of *Epha7* overexpression on limb innervation. Furthermore, the closely related *Epha4* gene has a similar expression pattern as compared to *Epha7* in the dorsal limbs, and an innervation defect limited to the hindlimbs (Helmbacher et al., 2000) suggesting the possibility of redundant function of *Epha4*/*Epha7* in the forelimb.

Proximal muscle patterning is perturbed in Shox2 mutants

Above, we used WISH to validate the differential expression of *Dmd* and *Meox1* (Figs. 4A–D), two genes known to be involved in myogenesis. Therefore we wanted to determine if *Shox2* deficiency resulted in muscle defects in developing forelimbs. We visualized muscle patterning with the MF20 antibody that recognizes myosin heavy chain in differentiating myocytes, which we first detected in forelimbs at E11.5 (Fig. 6A and Martin, 1990). In controls the first obvious muscle bundle formed in the proximal limb (Fig. 6A, arrow).

Fig. 5. The radial and axillary nerves are missing in *Shox2*-mutant forelimbs and their loss correlates with a gain in *Epha7* expression. (A–B) Side view, from the posterior, of E11.5 forelimb buds stained with the 2H3 anti-neurofilament antibody. Dorsal is above and ventral below. The dorsal nerve (bs—*brachialis superior*) is truncated abruptly in the mutant (arrowhead). This results in a complete absence of the radial (r) and axillary (a) nerve found in the control. In contrast the ulnar (u) and median nerves (m) develop similarly in both genotypes. (C–D) E11.5 WISH with an *Epha7* riboprobe. Limb buds are oriented as in A–B. The gain in mutant *Epha7* expression (arrow in D) compared to the control (C) is in the same region where the dorsal axons are truncated. (E–F) Dorsal view of the same limb buds from A–B. The radial nerve visible in the wildtype (r) is missing in the mutant as the dorsal limb branch is truncated at the level of the arrowhead. (G–H) *Epha7* WISH, dorsal view of the limb buds from C–D. Arrows indicate where *Epha7* is gained in the mutant, which corresponds to where the dorsal nerves are truncated in F. (I–J) E12.5 neurofilament staining. Axons from the radial nerve (r) are extending distally into the limb, but remain truncated in the mutant (arrowhead). Arrow in J indicates expected location of radial nerve. (K–L) E12.5 WISH detecting *Ednrb* transcripts. The radial (r) and axillary (a) nerves are clearly detected by this riboprobe in the control limbs (compare to I–J), but are missing in the mutant (L, arrow). (M–N) By E13.5 the axons of the radial nerve (arrow) are reaching the digits of the control limb (arrowhead). In contrast, the radial nerve (expected location indicated by the arrow) is missing from the mutant, but median (m) and ulnar (u) nerves appear normal.

Positive cells could also be seen more distally in the zeugopod region, but the region of the humerus was mostly devoid of myocytes (Fig. 6A, open arrow). In contrast, at E11.5 the limbs of *Shox2*$^{c/-}$ embryos showed no proximal muscle bundle (Fig. 6B, arrow) and had disorganized myocytes in the region of the humerus condensation (Fig. 6B, open arrow). This defect was observed in six of six mutant embryos stained.

At E12.5 muscle bundles were evident in the stylopod and zeugopod regions of the developing limb (Figs. 6C–D). Although all muscles were not yet distinct, many could be identified even at this early stage.

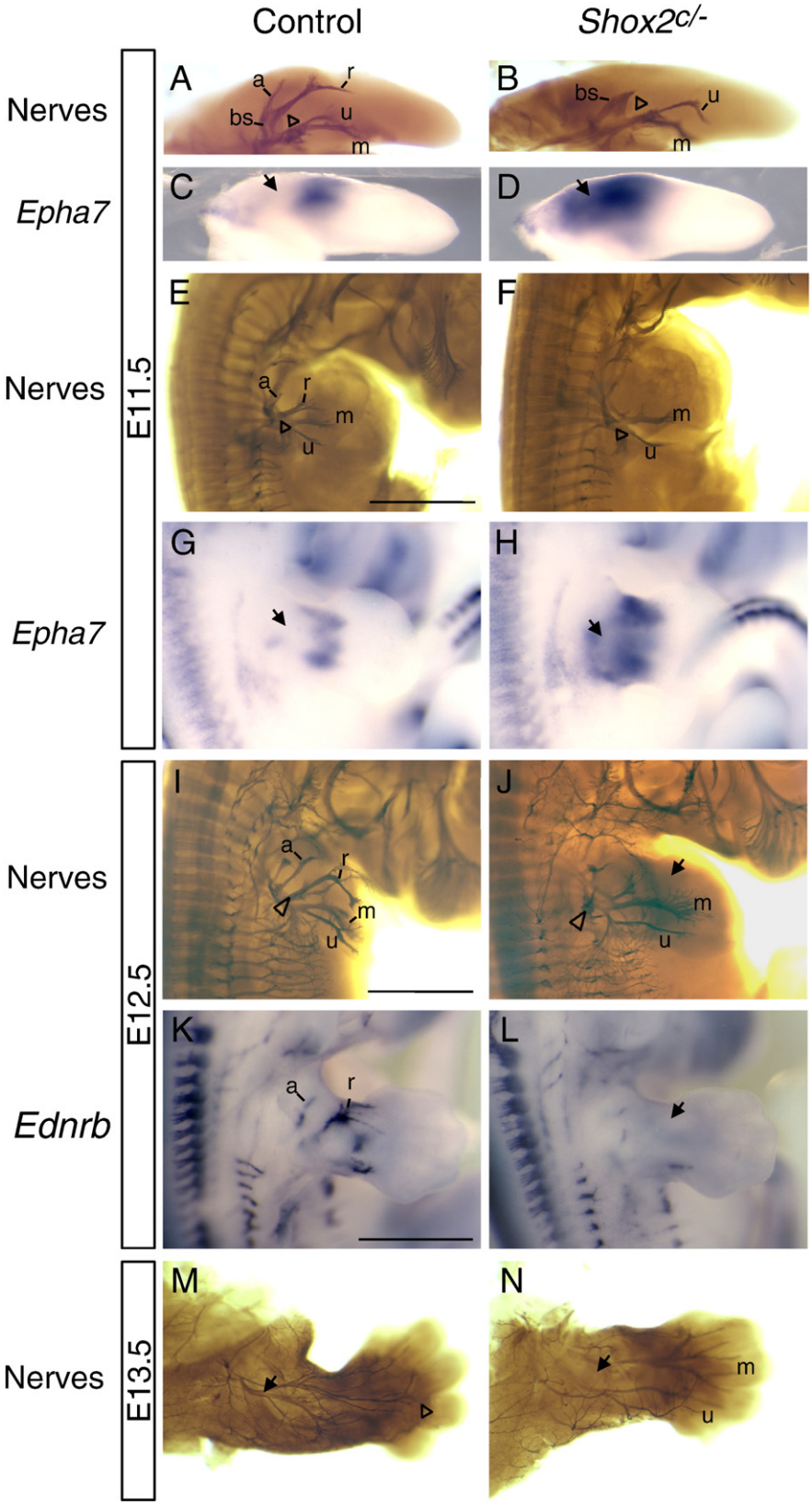

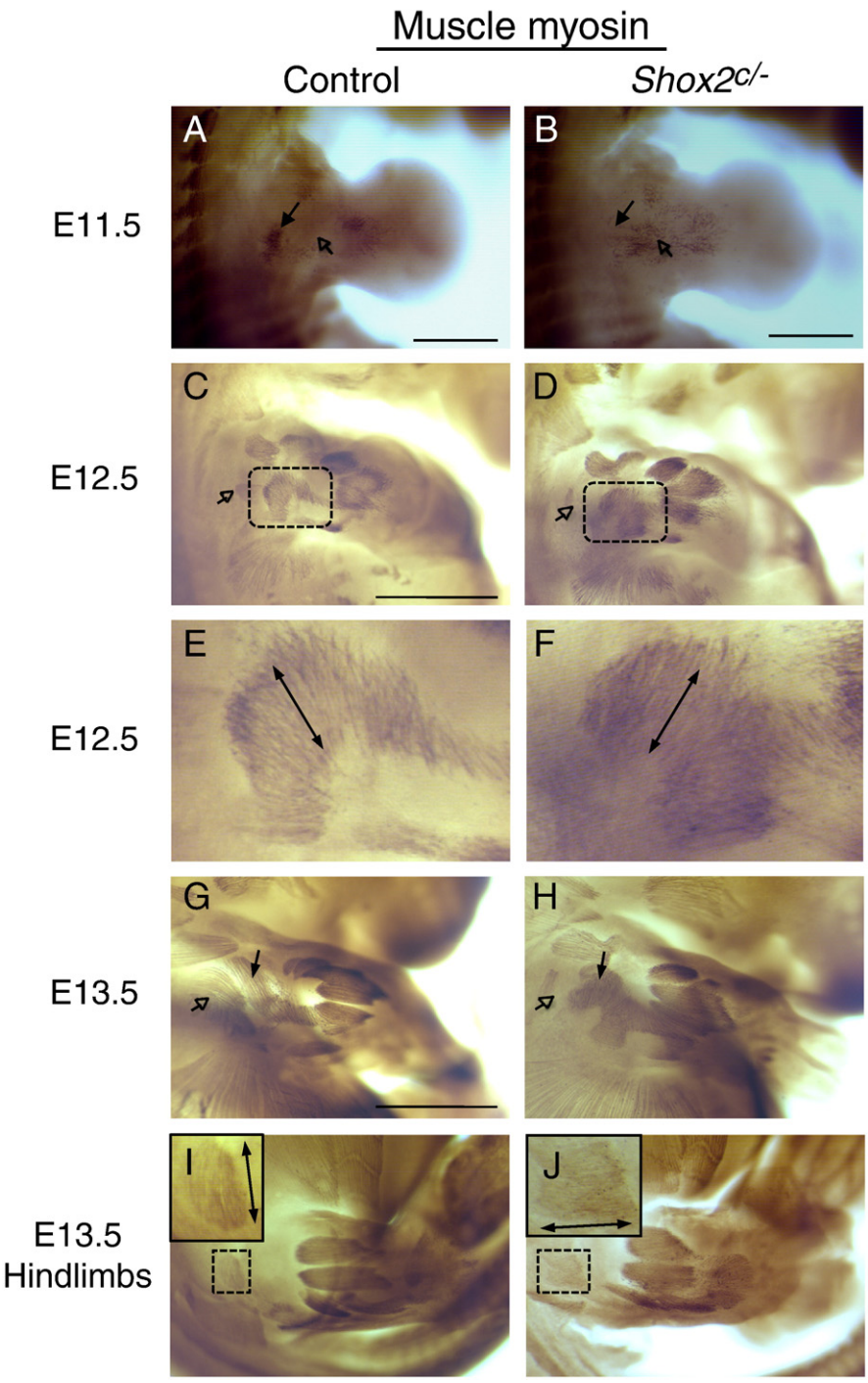

Fig. 6. Muscle patterning is abnormal in the proximal limbs of *Shox2* mutants. All images are of whole-mount immunohistochemistry with the MF20 antibody recognizing myosin heavy chain. (A–B) The proximal muscle bundle visible in control forelimbs at E11.5 is missing in the mutants (arrows). Instead muscle progenitors in the mutant are found in the region of the forming humerus where they are not found in wild-type forelimbs (open arrows). (C–D) The muscle filaments of the *T.b. lateralis* muscle (boxed) are roughly parallel to the humerus in the control limb (C), but are approximately orthogonal to this orientation in the mutant (D). The *T.b. longus* muscle is visible in the control limb (open arrow), but not in the mutant. The boxed regions are shown magnified in (E–F) with arrows indicating the orientation of the muscle fibers. (G–H) At E13.5 the *T.b. lateralis* muscle fibers are oriented abnormally in mutant forelimbs (arrows), and the *T.b. longus* is not visible in the mutant as it is in the control (open arrows). (I–J) In the hindlimbs at E13.5, the fibers of the muscle bundles forming the quadriceps muscles (boxed) are arranged approximately at right angles in the control (I) as compared to the mutant (J). Insets are magnified views of the boxed areas with arrows representing the orientation of muscle fibers. Scale bar represents 1 mm.

(Muscle anatomy was taken from the mouse limb anatomy atlas described in Delaurier et al. (2008).) We noted obvious abnormalities just posterior to the humerus in the forming triceps muscles. Specifically the fibers of the *Triceps brachii* (*T.b.*) *lateralis* (boxed in Figs. 6C–D) were arranged approximately orthogonally in the mutant compared to controls (Figs. 6E–F, arrows). This defect was also visible at E13.5 when the muscle bundles were more clearly defined (arrows in Figs. 6G–H). In controls, the *T.b. lateralis* muscle fibers were parallel to the humerus, which allows the fibers to function later in extending the forelimb at the elbow. Also at E13.5, the *T.b. longus* muscle formed parallel and posterior to the *T.b. lateralis* in controls but was not present in the mutant (Figs. 6G–H, open arrows). The absence of the *T.b. longus* muscle was apparent in $Shox2^{c/-}$ embryos as early as E12.5 (Figs. 6C–D, open arrows). Although it is not apparent until E13.5, the analogous

muscle bundles in the hindlimbs have a similar abnormality in *Shox2* mutants (Figs. 6I–J). The muscle fibers of the forming quadriceps muscles (*Vastus intermedius/lateralis/medialis*) are oriented at approximately right angles in mutants as compared to wild type hindlimbs at E13.5, similar to the triceps phenotype in forelimbs.

These data demonstrate that *Shox2* mutants have a failure in normal muscle formation from its earliest steps at E11.5. Skeletal defects are just beginning to appear at this same early stage; therefore it is unlikely that the muscle abnormalities are a secondary effect of the skeletal phenotype. A perturbed muscle pattern is already well established by E13.5, when a substantial humerus is still present in mutant fetuses (Cobb et al., 2006). The tissue phenotypes are reflected in the walking difficulties observed in $Shox2^{c/-}$ mice. These animals are not paralyzed, but their limbs move in a stiff, inefficient, "paddle-like" motion (see the Supplementary movie).

Discussion

The dissection of the transcriptional regulatory networks required for limb development is complicated by the underlying redundancy of many of the proteins involved. *Shox2*-mutant mice have proven a useful tool in this context since mutation of this single gene causes a severe phenotype. We have shown that specific gene expression patterns in the forelimb are dependent on *Shox2* as early as E10.5. By E11.5, muscle, skeletal and neural defects appear in the proximal forelimbs of *Shox2* mutants, suggesting a coupling of the developmental processes in the three tissues through the function of *Shox2*. The defects reported here could be linked to the gene expression changes described or other undetected downstream targets. Alternatively, the SHOX2 protein might have functions in addition to its predicted role as a DNA-binding transcription factor.

Shox2 is required to pattern the triceps muscles

The loss of *Meox1* expression provided an important clue that muscle patterning may be altered in *Shox2* mutants. Mice with null mutations for both *Meox1* and *Meox2* have a severe depletion of skeletal muscles including those in the limbs, demonstrating the necessity of these genes for myogenesis (Mankoo et al., 2003). Muscle precursors from the somites have been shown to arrive in the limb bud during the ninth day of development, but they do not activate the myogenic program until E11.5, as shown by *MyoD* expression (Sassoon et al., 1989). Evidence from the chick indicates that the subset of muscle precursors that express *Meox1* stop expressing this gene when they activate *MyoD* expression (Reijntjes et al., 2007). In *Shox2* mutants, these cells either fail to arrive in the region of the humerus or do not activate or maintain *Meox1* expression. These results, together with our detection of ectopic myogenic differentiation by an upregulation of *Dmd* (Fig. 4B) and an increase in myosin-positive cells (Fig. 6B) indicated an abnormal distribution of muscle precursors from an early stage in mutant limbs.

There is considerable evidence that the limb musculature develops by a non-autonomous mechanism in response to extrinsic cues in the mesenchyme that instruct the muscle precursor cells arriving from the somites to form the patterns of specific muscles (Chevallier et al., 1977; Kardon et al., 2002; Li et al., 2010). Nonetheless, we have not yet determined if this is the case for the *Shox2* patterning function. Although it is not expressed in the myotome or elsewhere in the somites, *Shox2* is expressed in embryonic and adult skeletal muscles of the proximal limb (Rovescalli et al., 1996; Blaschke et al., 1998). Therefore, *Shox2* could potentially function in a cell autonomous manner to pattern the triceps muscles. This can be tested in future experiments by deleting *Shox2* specifically in all muscle precursors using the $Pax3^{Cre}$ transgenic line (Engleka et al., 2005).

Wnt/β-catenin signaling is known to be one of the molecular signals in the mesenchyme required to pattern myogenic cells. Specifically, the transcription factor TCF4, a binding partner and cofactor for β-catenin, is expressed in domains that form a prepattern for the limb musculature (Kardon et al., 2003). Furthermore, conditional deletion of β-catenin in limb mesenchyme disrupts muscle patterning and causes ectopic muscle splitting (Hasson et al., 2010). β-Catenin's function as a cell adhesion molecule downstream of the TBX4/5 transcription factors is also required for muscle patterning (Hasson et al., 2010). Interestingly, the orientation of the *T.b. lateralis* in $Shox2^{c/-}$ limbs (Figs. 6D,F, and H) is similar to the same muscle in *Tbx5*-null limbs except in this latter case more muscles are affected (Hasson et al., 2010).

Because of the known role for β-catenin in muscle patterning, the increase in *Rspo3* expression we observed could be involved in disrupting muscle patterning in $Shox2^{c/-}$ forelimbs. *Rspo3* codes for one of four members of the R-spondin protein family that are secreted ligands for the Frizzled 8 and LRP6 receptors that activate Wnt/β-catenin signaling (Nam et al., 2006). *Rspo3* is required for angiogenesis in the early embryo in the placenta and yolk sac (Kazanskaya et al., 2008). Because of the early embryonic lethality of a null *Rspo3* mutation, a role in limb development has not been described. Although we observed a gain in *Rspo3* expression where ectopic myocytes were seen (Fig. 2H, compare with 6B), we have been unable to detect an increase in β-catenin signaling in $Shox2^{c/-}$ embryonic limbs using a *TCF-LacZ* reporter line (Mohamed et al., 2004) (data not shown). Interestingly *Rspo2* is required for *Xenopus* muscle development, thus establishing an intriguing link between R-spondins and myogenesis (Kazanskaya et al., 2004). Furthermore, the known role of Wnt-signaling in skeletal development (Hill et al., 2005) indicates the potential importance of modulating *Rspo3* during skeletal development.

Failure of dorsal innervation of the forelimb in the absence of Shox2

Our detection of a deficiency of *Ednrb* expression in $Shox2^{c/-}$ forelimbs led to the identification of an axonal pathfinding defect in these animals. Since the loss of *Ednrb* expression was presumably detected because its transcripts are found in axons or closely associated cells, *Ednrb* was likely a fortuitous indicator of the presence of axons. Since neural expression of *Shox2* is not affected in our conditional mutant (Fig. 1B), the axonal pathfinding defect implicates a function for SHOX2 in controlling the expression of extrinsic cues in the limb mesenchyme rather than intrinsic cues on axons. We correlated the loss of the radial and axillary nerves in *Shox2* mutants with a gain of *Epha7* expression in the limb bud. Interestingly, HOXD13 and HOXA13 have been shown to directly activate transcription of *Epha7* in developing limbs (Salsi and Zappavigna, 2006). Since SHOX2 has a repressive effect on *Epha7* expression, *Shox2* and *Hox* genes could antagonistically regulate *Epha7* expression in the limb mesenchyme. This is potentially significant since EphA receptors and their ephrin-A ligands are known to have critical roles in limb innervation. Furthermore, retinal axons have been shown to be repulsed by the EPHA7 protein (Rashid et al., 2005). EphA proteins are expressed on axons innervating the dorsal limb where they are repelled by ephrin-A5 in the ventral mesenchyme (Kania and Jessell, 2003). Therefore repulsion of Eph-bearing axons by ephrins in the limb mesenchyme mediates a key step in limb innervation. However, this binary choice is made near the beginning of an axon's journey into the limb bud. In the defect we describe the initial pathways were not affected since the *brachialis superior* forms dorsally as in controls (Figs. 5A–B). Only after this did axons in $Shox2^{c/-}$ mutants become truncated at a more dorsal position (Fig. 5B). Regardless of the specific molecules involved, the phenotype described here is an important tool for understanding later steps in limb innervation, after the dorsal/ventral choice mediated by mesenchymal ephrins and axonal Eph proteins.

In addition to repulsive and attractive cues, permissive interactions between the migrating axons and the ECM are likely to be

involved in the ultimate paths of the limb axons (Gundersen, 1987). The axons of the developing axillary and radial nerve develop in particularly close association with the humerus condensation as can be seen by comparing *Matn4* to *Ednrb* expression in Figs. 3A and C. These nerves curl over the dorsal aspect of the humerus and therefore presumably make close contact with the underlying ECM. *Matn4* codes for one of four matrilin proteins of mostly unknown function that are non-cartilage components of the ECM (Wagener et al., 2005). One matrilin family member, MATN2 has recently been shown to promote outgrowth of dorsal root ganglia axons and to be permissive for axon extension (Malin et al., 2009). If MATN4 has a similar function for limb axons, the lack of *Matn4* expression in the developing humerus (Fig. 3B) could leave migrating axons without a pathway to reach the distal limb, thus leaving them truncated.

Our data are consistent with a model in which projection of axons into the dorsal forelimb is dependent on extrinsic cues in the region of the developing humerus. To test if the candidates we have identified are important for this process, we will need to determine the role of *Matn4* in axonal pathfinding in the limb, and the effects of *Epha7* overexpression. Furthermore we cannot exclude that the muscle and nerve phenotypes are somehow causally linked, or that one phenotype is secondary to the other. To summarize the muscle and neural phenotypes of *Shox2* mutants, Figs. 7A–B show double staining of muscles and nerves at E12.5, illustrating the relative position of each tissue defect.

Differences in Shox2 patterning in forelimbs and hindlimbs, stylopod and zeugopod

The patterning function of *Shox2* in muscles and skeletal elements is very similar in the fore and hindlimbs. However this is not true for neural patterning since the dorsal innervation deficit is limited to the forelimb of *Shox2* mutants (Fig. 7). If one assumes that the skeletal condensations can influence axonal pathfinding, comparison of the geometry of fore and hindlimb innervation may explain this difference. Axons innervating the forelimb extend from a single plexus. To reach the anterior of the dorsal forelimb, axons from the brachial plexus must pass over the humerus condensation from the posterior and then curve anteriorly (Fig. 7A and Shearer, 1933). In contrast axons innervating the hindlimb extend from both an anterior (lumbar) and a posterior (sacral) plexus, and can therefore extend radially to innervate the anterior and posterior limb respectively without passing over the territory of the developing femur (Figs. 7C–D and Tarchini et al., 2005). Therefore, hindlimb innervation would not be expected to utilize permissive or attractive/repulsive cues from the developing femur, as the axons in question do not make close contact with this condensation. A similar mechanism could explain the lack of a ventral innervation phenotype in the forelimb since the median and ulnar nerves make minimal contact with the humerus condensation during their extension. Instead, during their early development these nerves extend posterior to the humerus and then adjacent to the radius and ulna condensations (Shearer, 1933), which are normal in *Shox2* mutants.

Another striking result is that the *Shox2*-mutant phenotype in the skeleton and muscles is restricted to the stylopod region even though *Shox2* is also expressed in the zeugopod (Fig. 1C). Likewise the expression differences of some of the candidate genes identified in this study also include the zeugopod domain (particularly *Rspo3*, *Dmd*, *Rsrc1* and *Epha7*). At this point we cannot explain the lack of an abnormal phenotype in this region. However, if we draw parallels to *Hox* genes, which have similar functions in patterning specific segments during limb development, it is not surprising that *Shox2* function is most important in the most proximal portion of its expression domain. *Hoxd11* for example is expressed in the zeugopod

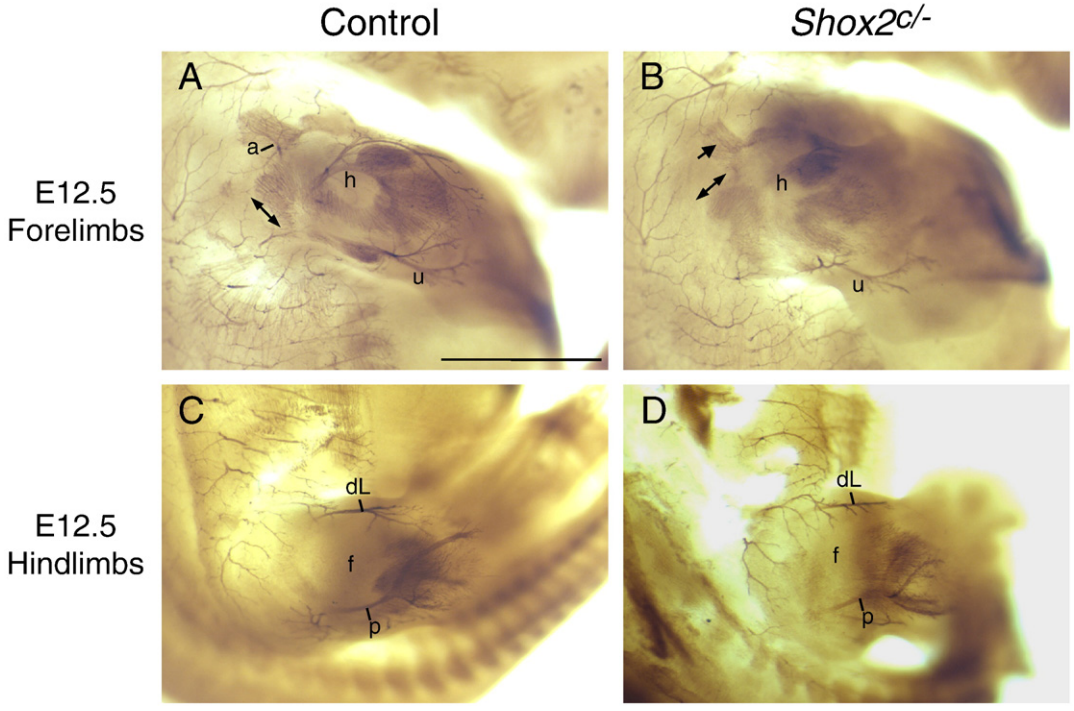

Fig. 7. The geometry of innervation and muscle development in forelimbs and hindlimbs. Neurofilament (2H3) and muscle (MF20) staining of dorsal limbs at E12.5 demonstrates the relative positions of the patterning defects in the different tissues. In the control forelimb (A) the radial nerve can be seen extending over the position of the humerus (h), but this nerve is not visible in the mutant (B) (expected position above the humerus (h)). (The position of skeletal elements can be inferred from comparison to Alcian blue-stained limbs, not shown). The double-headed arrows in A–B indicate the orientation of the triceps muscle fibers that are located more proximally and posteriorly than the affected radial and axillary nerves respectively. u = ulnar nerve, a = axillary nerve. The shoulder muscles innervated by the axillary nerve (a) in the control appear normal in the mutant (arrow) despite the absence of the axillary nerve at this position. In hindlimbs (C–D) innervation appears similar in controls and mutants. The peroneal nerve (p) extends radially from the sacral plexus into the posterior/dorsal hindlimb and the dorsal branch from the lumbar plexus (dL) extends into the anterior/dorsal domain. These nerves do not extend through the region of the developing femur (f).

and autopod, but its patterning function is limited to the zeugopod (Davis et al., 1995). Similarly *Shox2* may have redundant function with other genes in the zeugopod that mask its function in that domain.

Pheromones in limbs?

Undoubtedly the most surprising gene expression change we detected was that for *Mup1*. MUPs are known to function as pheromones/kairomones and as pheromone-binding proteins in both intra- and inter-specific communication (Chamero et al., 2007; Papes et al., 2010). Although it has no obvious connection to the patterning defects of *Shox2* mutants, the upregulation of *Mup1* is nonetheless striking for its precise location at the position of the humerus condensation. The *Mup* genes of the C57BL/6 genome consist of a cluster of 19 predicted genes and 18 pseudogenes on chromosome 4, but are represented by only a single pseudogene in humans (Mudge et al., 2008). The *Mup* complex is capable of prodigious transcription comprising an estimated 5% of mRNA in the adult male mouse liver (Shahan et al., 1987), which is reflected in the large amounts of MUP proteins in mouse urine. Embryonic expression for this gene complex has not been described previously. We suggest that the increase in *Mup* transcription may have no functional significance but could be detecting the signaling processes that are perturbed in the *Shox2*-mutant limb. As such, *Mup* transcription could serve as a tool for unraveling the processes involved in generating the *Shox2*-mutant phenotype.

Conclusion

Recent studies have demonstrated that muscle and skeletal patterning can be experimentally uncoupled (Hasson et al., 2010; Li et al., 2010), indicating that independent signaling mechanisms control each process. Similarly, nerves can innervate the limb in their normal pattern in the absence of muscles (Phelan and Hollyday, 1990). Nonetheless, these separate developmental processes must be coordinated to generate a functional limb with interacting axons, muscles and skeletal elements. Transcription factor proteins are obvious candidates for mediating the required synchronization of the development of the diverse tissues of the limb. To accomplish this, the spatiotemporally defined expression of different combinations of transcription factors, including *Shox2*, *Meis*, *Hox*, and *Tbx* genes, in different domains of the limbs must generate the precise expression patterns of downstream genes. As a step toward understanding these processes, we have demonstrated that *Shox2* is critical for coordinating the diverse processes of muscular, neural, and skeletal patterning in the proximal forelimb. The challenge now will be to determine how gene expression differences contribute to the tissue phenotypes described, and whether other transcription factors demonstrate a similar coupling of patterning processes. Also, the role of *Shox2* in the development of other tissues of the limb such as the vasculature and tendons should be investigated.

Supplementary materials related to this article can be found online at doi:10.1016/j.ydbio.2010.11.031.

Acknowledgments

We are grateful to D. Duboule for mice, support and consultations. We thank U. Drescher for the *Epha7*-mutant mice, D. Dufort and C. Schuurmans for *Tcf-LacZ* mice and P. Descombes, M. Docquier, and O. Schaad of the NCCR Genomics Platform, University of Geneva for microarray hybridization, data analysis and advice. We thank C. Ince for staining of the *Epha7*$^{-/-}$ embryos and X. Zhang for technical assistance and all members of the Cobb laboratory for discussions and critical comments on the manuscript. This work was supported in Geneva by funds from the Canton de Genève and the Swiss National Research Fund and in Calgary by the Natural Sciences and Engineering Research Council of Canada (NSERC) and the Canadian Institutes of Health Research (CIHR) Grant # MOP-93562. J.C. is supported as an Alberta Heritage Foundation for Medical Research (AHFMR) Scholar.

References

Bader, D., Masaki, T., Fischman, D.A., 1982. Immunochemical analysis of myosin heavy chain during avian myogenesis in vivo and in vitro. J. Cell Biol. 95, 763–770.
Blaschke, R.J., Hahurij, N.D., Kuijper, S., Just, S., Wisse, L.J., Deissler, K., Maxelon, T., Anastassiadis, K., Spitzer, J., Hardt, S.E., Scholer, H., Feitsma, H., Rottbauer, W., Blum, M., Meijlink, F., Rappold, G., Gittenberger-de Groot, A.C., 2007. Targeted mutation reveals essential functions of the homeodomain transcription factor Shox2 in sinoatrial and pacemaking development. Circulation 115, 1830–1838.
Blaschke, R.J., Monaghan, A.P., Schiller, S., Schechinger, B., Rao, E., Padilla-Nash, H., Ried, T., Rappold, G.A., 1998. SHOT, a SHOX-related homeobox gene, is implicated in craniofacial, brain, heart, and limb development. Proc. Natl. Acad. Sci. USA 95, 2406–2411.
Bult, C.J., Kadin, J.A., Richardson, J.E., Blake, J.A., Eppig, J.T., 2010. The Mouse Genome Database: enhancements and updates. Nucleic Acids Res. 38, D586–D592.
Chamero, P., Marton, T.F., Logan, D.W., Flanagan, K., Cruz, J.R., Saghatelian, A., Cravatt, B.F., Stowers, L., 2007. Identification of protein pheromones that promote aggressive behaviour. Nature 450, 899–902.
Chevallier, A., Kieny, M., Mauger, A., 1977. Limb–somite relationship: origin of the limb musculature. J. Embryol. Exp. Morphol. 41, 245–258.
Clement-Jones, M., Schiller, S., Rao, E., Blaschke, R.J., Zuniga, A., Zeller, R., Robson, S.C., Binder, G., Glass, I., Strachan, T., Lindsay, S., Rappold, G.A., 2000. The short stature homeobox gene SHOX is involved in skeletal abnormalities in Turner syndrome. Hum. Mol. Genet. 9, 695–702.
Cobb, J., Dierich, A., Huss-Garcia, Y., Duboule, D., 2006. A mouse model for human short-stature syndromes identifies Shox2 as an upstream regulator of Runx2 during long-bone development. Proc. Natl. Acad. Sci. USA 103, 4511–4515.
Cobb, J., Duboule, D., 2005. Comparative analysis of genes downstream of the Hoxd cluster in developing digits and external genitalia. Development 132, 3055–3067.
Davis, A.P., Witte, D.P., Hsieh-Li, H.M., Potter, S.S., Capecchi, M.R., 1995. Absence of radius and ulna in mice lacking hoxa-11 and hoxd-11. Nature 375, 791–795.
Delaurier, A., Burton, N., Bennett, M., Baldock, R., Davidson, D., Mohun, T.J., Logan, M.P., 2008. The Mouse Limb Anatomy Atlas: an interactive 3D tool for studying embryonic limb patterning. BMC Dev. Biol. 8, 83.
Dodd, J., Morton, S.B., Karagogeos, D., Yamamoto, M., Jessell, T.M., 1988. Spatial regulation of axonal glycoprotein expression on subsets of embryonic spinal neurons. Neuron 1, 105–116.
Duprez, D., 2002. Signals regulating muscle formation in the limb during embryonic development. Int. J. Dev. Biol. 46, 915–925.
Engleka, K.A., Gitler, A.D., Zhang, M., Zhou, D.D., High, F.A., Epstein, J.A., 2005. Insertion of Cre into the Pax3 locus creates a new allele of Splotch and identifies unexpected Pax3 derivatives. Dev. Biol. 280, 396–406.
Graves, J.A., Wakefield, M.J., Toder, R., 1998. The origin and evolution of the pseudoautosomal regions of human sex chromosomes. Hum. Mol. Genet. 7, 1991–1996.
Gundersen, R.W., 1987. Response of sensory neurites and growth cones to patterned substrata of laminin and fibronectin in vitro. Dev. Biol. 121, 423–431.
Hasson, P., DeLaurier, A., Bennett, M., Grigorieva, E., Naiche, L.A., Papaioannou, V.E., Mohun, T.J., Logan, M.P., 2010. Tbx4 and tbx5 acting in connective tissue are required for limb muscle and tendon patterning. Dev. Cell 18, 148–156.
Helmbacher, F., Schneider-Maunoury, S., Topilko, P., Tiret, L., Charnay, P., 2000. Targeting of the EphA4 tyrosine kinase receptor affects dorsal/ventral pathfinding of limb motor axons. Development 127, 3313–3324.
Hill, T.P., Spater, D., Taketo, M.M., Birchmeier, W., Hartmann, C., 2005. Canonical Wnt/beta-catenin signaling prevents osteoblasts from differentiating into chondrocytes. Dev. Cell 8, 727–738.
Hisa, T., Spence, S.E., Rachel, R.A., Fujita, M., Nakamura, T., Ward, J.M., Devor-Henneman, D.E., Saiki, Y., Kutsuna, H., Tessarollo, L., Jenkins, N.A., Copeland, N.G., 2004. Hematopoietic, angiogenic and eye defects in Meis1 mutant animals. EMBO J. 23, 450–459.
Houzelstein, D., Lyons, G.E., Chamberlain, J., Buckingham, M.E., 1992. Localization of dystrophin gene transcripts during mouse embryogenesis. J. Cell Biol. 119, 811–821.
Hubbell, E., Liu, W.M., Mei, R., 2002. Robust estimators for expression analysis. Bioinformatics 18, 1585–1592.
Hutcheson, D.A., Zhao, J., Merrell, A., Haldar, M., Kardon, G., 2009. Embryonic and fetal limb myogenic cells are derived from developmentally distinct progenitors and have different requirements for beta-catenin. Genes Dev. 23, 997–1013.
Kania, A., Jessell, T.M., 2003. Topographic motor projections in the limb imposed by LIM homeodomain protein regulation of ephrin-A:EphA interactions. Neuron 38, 581–596.
Kardon, G., Campbell, J.K., Tabin, C.J., 2002. Local extrinsic signals determine muscle and endothelial cell fate and patterning in the vertebrate limb. Dev. Cell 3, 533–545.
Kardon, G., Harfe, B.D., Tabin, C.J., 2003. A Tcf4-positive mesodermal population provides a prepattern for vertebrate limb muscle patterning. Dev. Cell 5, 937–944.
Kask, K., Zamanillo, D., Rozov, A., Burnashev, N., Sprengel, R., Seeburg, P.H., 1998. The AMPA receptor subunit GluR-B in its Q/R site-unedited form is not essential for brain development and function. Proc. Natl. Acad. Sci. USA 95, 13777–13782.

Kazanskaya, O., Glinka, A., del Barco Barrantes, I., Stannek, P., Niehrs, C., Wu, W., 2004. R-Spondin2 is a secreted activator of Wnt/beta-catenin signaling and is required for Xenopus myogenesis. Dev. Cell 7, 525–534.
Kazanskaya, O., Ohkawara, B., Heroult, M., Wu, W., Maltry, N., Augustin, H.G., Niehrs, C., 2008. The Wnt signaling regulator R-spondin 3 promotes angioblast and vascular development. Development 135, 3655–3664.
Kmita, M., Tarchini, B., Zakany, J., Logan, M., Tabin, C.J., Duboule, D., 2005. Early developmental arrest of mammalian limbs lacking HoxA/HoxD gene function. Nature 435, 1113–1116.
Le Martelot, G., Claudel, T., Gatfield, D., Schaad, O., Kornmann, B., Sasso, G.L., Moschetta, A., Schibler, U., 2009. REV-ERBalpha participates in circadian SREBP signaling and bile acid homeostasis. PLoS Biol. 7, e1000181.
Lee, H.O., Levorse, J.M., Shin, M.K., 2003. The endothelin receptor-B is required for the migration of neural crest-derived melanocyte and enteric neuron precursors. Dev. Biol. 259, 162–175.
Li, Y., Qiu, Q., Watson, S.S., Schweitzer, R., Johnson, R.L., 2010. Uncoupling skeletal and connective tissue patterning: conditional deletion in cartilage progenitors reveals cell-autonomous requirements for Lmx1b in dorsal–ventral limb patterning. Development 137, 1181–1188.
Liu, W.M., Mei, R., Di, X., Ryder, T.B., Hubbell, E., Dee, S., Webster, T.A., Harrington, C.A., Ho, M.H., Baid, J., Smeekens, S.P., 2002. Analysis of high density expression microarrays with signed-rank call algorithms. Bioinformatics 18, 1593–1599.
Luria, V., Krawchuk, D., Jessell, T.M., Laufer, E., Kania, A., 2008. Specification of motor axon trajectory by ephrin-B:EphB signaling: symmetrical control of axonal patterning in the developing limb. Neuron 60, 1039–1053.
Malin, D., Sonnenberg-Riethmacher, E., Guseva, D., Wagener, R., Aszodi, A., Irintchev, A., Riethmacher, D., 2009. The extracellular-matrix protein matrilin 2 participates in peripheral nerve regeneration. J. Cell Sci. 122, 995–1004.
Mankoo, B.S., Skuntz, S., Harrigan, I., Grigorieva, E., Candia, A., Wright, C.V., Arnheiter, H., Pachnis, V., 2003. The concerted action of Meox homeobox genes is required upstream of genetic pathways essential for the formation, patterning and differentiation of somites. Development 130, 4655–4664.
Martin, P., 1990. Tissue patterning in the developing mouse limb. Int. J. Dev. Biol. 34, 323–336.
Meijlink, F., Beverdam, A., Brouwer, A., Oosterveen, T.C., Berge, D.T., 1999. Vertebrate aristaless-related genes. Int. J. Dev. Biol. 43, 651–663.
Mercader, N., Leonardo, E., Azpiazu, N., Serrano, A., Morata, G., Martinez, C., Torres, M., 1999. Conserved regulation of proximodistal limb axis development by Meis1/Hth. Nature 402, 425–429.
Mercader, N., Selleri, L., Criado, L.M., Pallares, P., Parras, C., Cleary, M.L., Torres, M., 2009. Ectopic Meis1 expression in the mouse limb bud alters P–D patterning in a Pbx1-independent manner. Int. J. Dev. Biol. 53, 1483–1494.
Mohamed, O.A., Clarke, H.J., Dufort, D., 2004. Beta-catenin signaling marks the prospective site of primitive streak formation in the mouse embryo. Dev. Dyn. 231, 416–424.
Mudge, J.M., Armstrong, S.D., McLaren, K., Beynon, R.J., Hurst, J.L., Nicholson, C., Robertson, D.H., Wilming, L.G., Harrow, J.L., 2008. Dynamic instability of the major urinary protein gene family revealed by genomic and phenotypic comparisons between C57 and 129 strain mice. Genome Biol. 9, R91.
Nam, J.S., Turcotte, T.J., Smith, P.F., Choi, S., Yoon, J.K., 2006. Mouse cristin/R-spondin family proteins are novel ligands for the Frizzled 8 and LRP6 receptors and activate beta-catenin-dependent gene expression. J. Biol. Chem. 281, 13247–13257.
Nef, S., Schaad, O., Stallings, N.R., Cederroth, C.R., Pitetti, J.L., Schaer, G., Malki, S., Dubois-Dauphin, M., Boizet-Bonhoure, B., Descombes, P., Parker, K.L., Vassalli, J.D., 2005. Gene expression during sex determination reveals a robust female genetic program at the onset of ovarian development. Dev. Biol. 287, 361–377.
Papes, F., Logan, D.W., Stowers, L., 2010. The vomeronasal organ mediates interspecies defensive behaviors through detection of protein pheromone homologs. Cell 141, 692–703.
Phelan, K.A., Hollyday, M., 1990. Axon guidance in muscleless chick wings: the role of muscle cells in motoneuronal pathway selection and muscle nerve formation. J. Neurosci. 10, 2699–2716.
Rao, E., Weiss, B., Fukami, M., Rump, A., Niesler, B., Mertz, A., Muroya, K., Binder, G., Kirsch, S., Winkelmann, M., Nordsiek, G., Heinrich, U., Breuning, M.H., Ranke, M.B., Rosenthal, A., Ogata, T., Rappold, G.A., 1997. Pseudoautosomal deletions encompassing a novel homeobox gene cause growth failure in idiopathic short stature and Turner syndrome. Nat. Genet. 16, 54–63.
Rashid, T., Upton, A.L., Blentic, A., Ciossek, T., Knoll, B., Thompson, I.D., Drescher, U., 2005. Opposing gradients of ephrin-As and EphA7 in the superior colliculus are essential for topographic mapping in the mammalian visual system. Neuron 47, 57–69.
Reijntjes, S., Stricker, S., Mankoo, B.S., 2007. A comparative analysis of Meox1 and Meox2 in the developing somites and limbs of the chick embryo. Int. J. Dev. Biol. 51, 753–759.
Rovescalli, A.C., Asoh, S., Nirenberg, M., 1996. Cloning and characterization of four murine homeobox genes. Proc. Natl. Acad. Sci. USA 93, 10691–10696.
Salsi, V., Vigano, M.A., Cocchiarella, F., Mantovani, R., Zappavigna, V., 2008. Hoxd13 binds in vivo and regulates the expression of genes acting in key pathways for early limb and skeletal patterning. Dev. Biol. 317, 497–507.
Salsi, V., Zappavigna, V., 2006. Hoxd13 and Hoxa13 directly control the expression of the EphA7 Ephrin tyrosine kinase receptor in developing limbs. J. Biol. Chem. 281, 1992–1999.
Sassoon, D., Lyons, G., Wright, W.E., Lin, V., Lassar, A., Weintraub, H., Buckingham, M., 1989. Expression of two myogenic regulatory factors myogenin and MyoD1 during mouse embryogenesis. Nature 341, 303–307.
Semina, E.V., Reiter, R.S., Murray, J.C., 1998. A new human homeobox gene OGI2X is a member of the most conserved homeobox gene family and is expressed during heart development in mouse. Hum. Mol. Genet. 7, 415–422.
Shahan, K., Denaro, M., Gilmartin, M., Shi, Y., Derman, E., 1987. Expression of six mouse major urinary protein genes in the mammary, parotid, sublingual, submaxillary, and lachrymal glands and in the liver. Mol. Cell. Biol. 7, 1947–1954.
Shearer, E.M., 1933. The development of the arteries in the anterior limb of the albino rat. Am. J. Anat. 53, 427–467.
Shears, D.J., Vassal, H.J., Goodman, F.R., Palmer, R.W., Reardon, W., Superti-Furga, A., Scambler, P.J., Winter, R.M., 1998. Mutation and deletion of the pseudoautosomal gene SHOX cause Leri–Weill dyschondrosteosis. Nat. Genet. 19, 70–73.
Shukunami, C., Iyama, K., Inoue, H., Hiraki, Y., 1999. Spatiotemporal pattern of the mouse chondromodulin-I gene expression and its regulatory role in vascular invasion into cartilage during endochondral bone formation. Int. J. Dev. Biol. 43, 39–49.
Tarchini, B., Huynh, T.H., Cox, G.A., Duboule, D., 2005. HoxD cluster scanning deletions identify multiple defects leading to paralysis in the mouse mutant Ironside. Genes Dev. 19, 2862–2876.
Tickle, C., 2003. Patterning systems—from one end of the limb to the other. Dev. Cell 4, 449–458.
Wagener, R., Ehlen, H.W., Ko, Y.P., Kobbe, B., Mann, H.H., Sengle, G., Paulsson, M., 2005. The matrilins—adaptor proteins in the extracellular matrix. FEBS Lett. 579, 3323–3329.
Wellik, D.M., Capecchi, M.R., 2003. Hox10 and Hox11 genes are required to globally pattern the mammalian skeleton. Science 301, 363–367.
Zakany, J., Duboule, D., 2007. The role of Hox genes during vertebrate limb development. Curr. Opin. Genet. Dev. 17, 359–366.
Zeller, R., Lopez-Rios, J., Zuniga, A., 2009. Vertebrate limb bud development: moving towards integrative analysis of organogenesis. Nat. Rev. Genet. 10, 845–858.
Zinn, A.R., Wei, F., Zhang, L., Elder, F.F., Scott Jr., C.I., Marttila, P., Ross, J.L., 2002. Complete SHOX deficiency causes Langer mesomelic dysplasia. Am. J. Med. Genet. 110, 158–163.